

Polarization response of spin-lasers under amplitude modulation

Gaofeng Xu,^{1,*} Krish Patel,² and Igor Žutić^{2,†}

¹*Department of Physics, Hangzhou Dianzi University, Hangzhou, Zhejiang 310018, China*

²*Department of Physics, University at Buffalo, State University of New York, Buffalo, NY 14260, USA*

Lasers with injected spin-polarized carriers show an outstanding performance in both static and dynamic operation. In addition to the intensity response of conventional lasers, without spin-polarized carriers, both intensity and polarization of light can be exploited for optical communication in spin-lasers. However, the polarization dynamics of spin-lasers under amplitude modulation has been largely overlooked. Here we reveal, analytically and numerically, a nontrivial polarization response that accompanies the well-known intensity dynamics of a spin-laser under amplitude modulation. We evaluate the polarization and intensity response under the same amplitude modulation, and further assess the capability of such a polarization response in digital data transfer with eye diagram simulations. Our results provide a more complete understanding of the modulation response in spin-lasers and open up unexplored opportunities in optical communication and spintronics.

Lasers are key devices in optical communication networks [1–4], typically using the intensity of the emitted light under amplitude modulation (AM) [5]. However, injecting spin-polarized carriers into the lasers gives rise to new opportunities, which can improve their performance in both static and dynamic operation, including reduced lasing threshold and enhanced modulation bandwidth [6–19]. In such spin-lasers, through conservation of angular momentum, the spin polarization of carriers can be converted into the circular polarization of the emitted light, which enables control and modulation of the polarization of emission and leads to room-temperature spintronic applications beyond magnetoresistance [20–28].

In a typical polarization modulation (PM) scheme, the spin-polarized injection can be modulated electrically or optically, which leads to a modulation of carrier spin polarization and the circularly polarized emitted light [18, 29–32]. For a spin-laser with large birefringence, the response of the circular polarization of light under polarization modulation has been shown to support a significantly enhanced modulation bandwidth and is promising for future ultrafast optical communication [18, 31–41].

Surprisingly, the dynamic response of the circularly polarized light in a spin-laser under AM has been largely overlooked, while a static regime was briefly considered [42]. In fact, a modulation of the total amplitude of spin-polarized injection changes both intensities of light helicities (left and right circularly polarized light), as well as their relative ratio, which leads to a time-varying circular polarization of the laser emission, shown in Fig. 1. With the current focus on adding spin-polarized carriers to vertical cavity surface emitting lasers (VCSELs) [3], employing experimentally simpler AM could be an important step towards realizing their dynamical operation at room temperature with electrical spin injection. This breakthrough could overcome the present limitation of a high-speed and low-power operation constrained to optically-injected spin-lasers [18].

Motivated by this situation, we investigate a nontrivial polarization response of a spin-laser under AM and

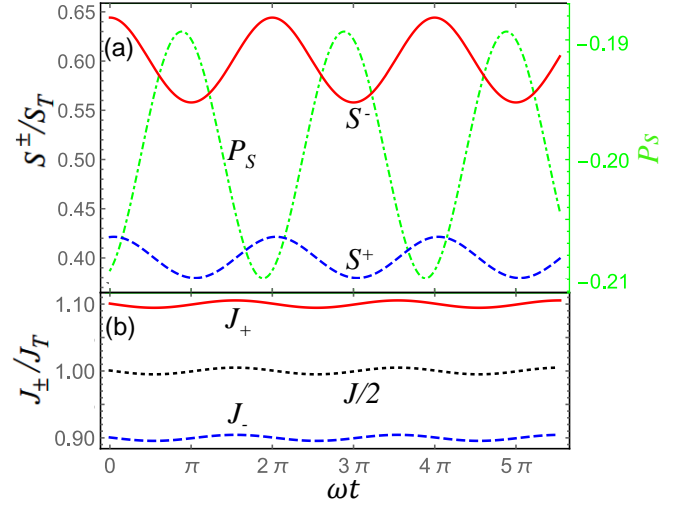


FIG. 1. Time evolution of (a) polarized light intensities S^\pm and polarization P_s , (b) spin-polarized injection J_\pm and their mean value $J/2$ under amplitude modulation. Light intensities are normalized to the intensity S_T at twice the threshold $2J_T$. The injection $J_0 = 2J_T$ with a constant spin polarization $P_J = 0.1$, and the modulation frequency and amplitude are $\omega/2\pi = 12$ GHz and $\delta J = 0.01J_T$, respectively.

explore the potential of such a response in digital communication. We use the rate equations for spin-lasers [6–8, 30, 43–45], which can be expressed in terms of spin- or helicity-resolved quantities [30, 43],

$$dn_\pm/dt = J_\pm - g_\pm S^\mp - (n_\pm - n_\mp)/\tau_s - R_{sp}^\pm, \quad (1)$$

$$dS^\pm/dt = \Gamma g_\mp S^\pm - S^\pm/\tau_{ph} + \beta \Gamma R_{sp}^\mp, \quad (2)$$

where n_\pm are the densities of spin-up (down) + (–) electrons (total $n = n_+ + n_-$), with a spin-relaxation time τ_s . Since holes typically have much shorter spin-relaxation times than those of electrons [20], only the electrons are spin polarized, while charge neutrality yields the densities of holes $p_\pm = (n_+ + n_-)/2$. J_\pm , where $J = J_+ + J_-$, are the injection rates of spin-up (down) + (–) electrons. S^\pm , where $S = S^+ + S^-$, are the photon densities of positive (+) and negative (–) helicity. We also introduce

the polarization of the injection, $P_J = (J_+ - J_-)/J$, and the emitted light, $P_S = (S^+ - S^-)/S$. The spontaneous recombination of carriers can be expressed in a linear form as $R_{sp}^\pm = n_\pm/\tau_r$, characterized by a carrier recombination time τ_r [43, 46, 47]. The spin-dependent optical gain, g_\pm can have various dependence on the carrier density [48]. In a linear model, it takes the form $g_\pm = g_0(n_\pm + p_\pm - n_{\text{tran}})$ [43], with g_0 the gain parameter and n_{tran} the transparency carrier density. Γ is the optical confinement factor and τ_{ph} is the photon lifetime in the cavity. The spontaneous emission factor $\beta \sim 10^{-5} - 10^{-3}$ [7, 8], characterizes the fraction of spontaneous emission coupled to the lasing mode.

We first consider a small-signal analysis (SSA) for a spin-laser under AM. The resulting decomposition $X(t) = X_0 + \delta X(t)$, into a steady-state and a small modulated part, is applied for J_\pm , n_\pm and S^\pm . The modulated quantities take the form $\delta X(t) = \text{Re}[\delta X_\omega e^{i\omega t}]$, where ω is the angular modulation frequency. Under AM, $J = J_0 + \delta J \cos \omega t$, with $P_J = P_{J0}$, such that $J_\pm = (1 \pm P_J)J/2$. Due to the simultaneous existence of n_\pm and p_\pm , an analytical solution of SSA is very lengthy.

To retain the analytical understanding, which still captures the main trends, we consider a simplified linear gain model $g_\pm = g_0(n_\pm - n_{\text{tran}}/2)$. In the limit of a long spin-relaxation time, $\tau_s \gg \tau_r$, we obtain

$$\delta S_\omega^\pm = \frac{(g_0 S_0^\pm + \beta/\tau_r)\delta J_\mp}{\frac{W_\pm}{\tau_r} + \frac{\beta G_0^\mp}{\tau_r} + g_0 G_0^\mp S_0^\pm + g_0 S_0^\pm W_\mp - i\omega W_\mp}, \quad (3)$$

where, we define $G_0^\pm \equiv g_0(n_{0\pm} - n_{\text{tran}}/2)$ and $W_\pm \equiv (-i\omega - \Gamma G_0^\pm + 1/\tau_{ph})/\Gamma$. Therefore, the resonance frequencies, ω_R^\pm , for δS^\pm , up to the linear order in β , are

$$\omega_R^\pm \approx \frac{g_0 S_0^\pm}{\tau_{ph}} - \frac{(\frac{1}{\tau_r} + g_0 S_0^\pm)^2}{2} - \frac{\beta}{\tau_r}(\Gamma g_0 n_{0\mp} - \frac{1}{\tau_{ph}}), \quad (4)$$

where the steady-state relation $1/\tau_{ph} - \Gamma G_0^\pm = \Gamma \beta n_{0\pm}/(S_0^\mp \tau_r)$ has been used. For $\beta \rightarrow 0$, we obtain

$$\delta S_\omega^\pm \approx \frac{\Gamma g_0 S_0^\pm \delta J_\mp}{-\omega^2 - i\omega(1/\tau_r + g_0 S_0^\pm) + g_0 S_0^\pm/\tau_{ph}}, \quad (5)$$

which, for $P_J = 0$, reduces to the result from conventional lasers [1]. The corresponding resonance frequencies become $\omega_R^\pm = \sqrt{g_0 S_0^\pm/\tau_{ph} - (1/\tau_r + g_0 S_0^\pm)^2/2}$.

We next analyze the time evolution of the circular polarization of the emitted light, P_S . We denote the complex amplitude as $\delta S_\omega^\pm = |\delta S_\omega^\pm| e^{i\phi_\pm}$, where

$$|\delta S_\omega^\pm| = \frac{\Gamma g_0 S_0^\pm \delta J_\mp}{\sqrt{(\omega^2 - g_0 S_0^\pm/\tau_{ph})^2 + \omega^2(1/\tau_r + g_0 S_0^\pm)^2}}, \quad (6)$$

$$\tan \phi_\pm = \omega(1/\tau_r + g_0 S_0^\pm)/(-\omega^2 + g_0 S_0^\pm/\tau_{ph}). \quad (7)$$

P_S can be generally expressed as

$$P_S(t) = \frac{S_0^+ - S_0^- + \delta S^+(t) - \delta S^-(t)}{S_0^+ + S_0^- + \delta S^+(t) + \delta S^-(t)}, \quad (8)$$

where $\delta S^\pm(t) = |\delta S_\omega^\pm| \cos(\omega t + \phi_\pm)$, or decomposed as $P_S(t) = P_S^0 + \delta P_S(t)$, where $P_S^0 = (S_0^+ - S_0^-)/S_0$, with $S_0 = S_0^+ + S_0^-$. For SSA, $|\delta S_\omega^\pm| \ll S_0$, therefore

$$\delta P_S(t) \approx \frac{|\delta S_\omega^+| \cos(\omega t + \phi_+) - |\delta S_\omega^-| \cos(\omega t + \phi_-)}{S_0}. \quad (9)$$

This AM response describes the results from Fig. 1 with $P_J = 0.1$, $\omega/2\pi = 12$ GHz, and $\delta J = 0.01J_T$. Unless otherwise specified, the parameters in our calculations are guided by the fabricated spin-VCSELs [7, 8, 30, 45]: $\Gamma = 0.029$, $n_{\text{tran}} = 4.0 \times 10^{17} \text{ cm}^{-3}$, $\tau_r = 200$ ps, $\tau_{ph} = 1.0$ ps, $\tau_s = 200$ ps, and $g_0 = 1.0 \times 10^{-5} \text{ cm}^3 \text{ s}^{-1}$. S^\pm undergo sinusoidal oscillations with separate mean values and the variation of S^+/S^- due to $P_J \neq 0$, which leads to oscillations, $\delta P_S(t) = A \cos(\omega t + \varphi)$, around $P_{S0} = -0.2$. In conventional lasers, $P_J = 0$ implies $P_S = 0$. The polarization oscillation amplitude of the emitted light is

$$A = \sqrt{A_+^2 + A_-^2 + 2A_+A_- \cos(\phi_+ - \phi_-)}, \quad (10)$$

$A_\pm = |\delta S_\omega^\pm|/S_0$ gives the superposition of two harmonic oscillations, $S_0^+ \neq S_0^-$, $|\delta S_\omega^+| \neq |\delta S_\omega^-|$ and $\phi_+ \neq \phi_-$.

This picture of the two harmonic oscillations also characterizes the AM results in Fig. 2 for the response of

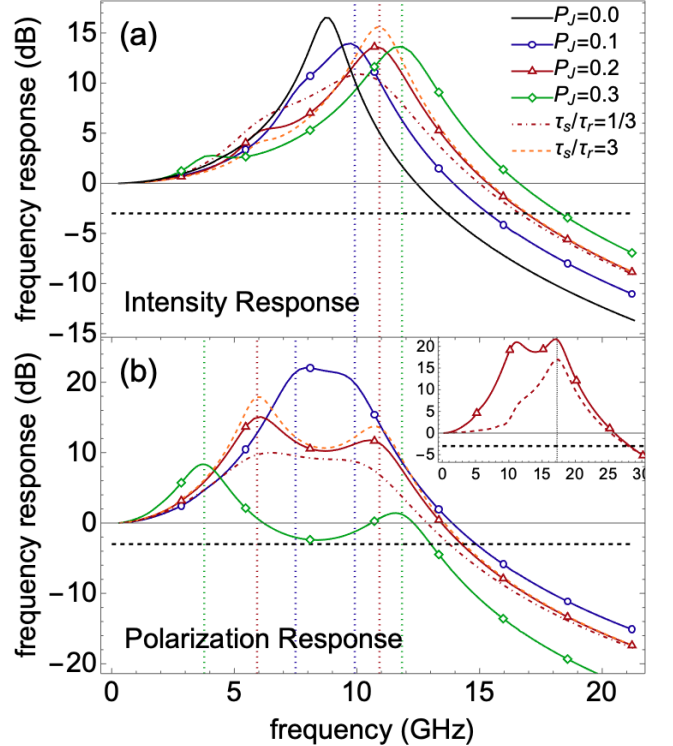


FIG. 2. AM: (a) Intensity and (b) polarization response. $P_J = 0.1, 0.2$, and 0.3 . $\tau_s/\tau_r = 1$, except for $\tau_s/\tau_r = 1/3$ and 3 with $P_J = 0.2$. $J_0 = 3J_T$, $\beta = 10^{-4}$. The simplified model $g_\pm = g_0(n_\pm - n_{\text{tran}}/2)$ is used. Vertical dashed lines: the resonance frequencies given by Eq. (4). Horizontal dashed lines: the -3 dB response, which indicate the modulation bandwidth. Inset: the polarization (solid) and intensity (dashed) response with the full linear gain model for $P_J = 0.2$.

S^- (majority spin) and P_S . The intensity response function, $R(f) = \delta S^- / \delta J_+$ [30], for $P_J \rightarrow 0$ reduces to the usual form, $R(f) = \delta S / \delta J$, in conventional lasers [1]. In contrast, the polarization response function, $R(f) = \delta P_S / \delta J$, has no conventional counterpart. Here δS^- and δP_S are the amplitudes of the intensity and polarization responses. These responses are normalized to their low-frequency values, f_{low} , as $\bar{R}(f) = 10 \log_{10}[R^2(f)/R^2(f_{\text{low}})]$.

While the intensity response peak in Fig. 2(a) is near $\omega = \omega_R^-$, given by Eq. (4), and shows an enhanced ω_R^- with P_J [30], the polarization response in Fig. 2(b) reveals the presence of two peaks. This can be understood because the amplitude of P_S oscillations involves contribution from both A_{\pm} , as given in Eq. 10, with unequal resonance frequencies, $\omega_R^+ \neq \omega_R^-$. Near ω_R^+ (ω_R^-), the amplitude A_+ (A_-) reaches its maximum value, which results in the lower (higher) peak of a frequency response in Fig. 2(b). ω_R^{\pm} from Eq. (4) are marked by vertical dashed lines, which coincide with the peaks of the intensity and polarization responses, showing a good agreement between analytical and numerical results, in which we also use a simplified gain model, $g_{\pm} = g_0(n_{\pm} - n_{\text{tran}}/2)$. However, this obtained agreement and the main trends in the frequency responses are not limited to the simplified gain model. Even with a more general model, $g_{\pm} = g_0(n_{\pm} + p_{\pm} - n_{\text{tran}})$, the results from the inset of Fig. 2(b) for $P_J = 0.2$ confirm a similar behavior in the frequency responses, only with slightly shifted resonant frequencies, justifying our use of a simplified gain model.

Since the electron spin-relaxation time, τ_s , is a key quantity that affects polarization response, it is important to understand its role on the modulation bandwidth, $f_{3\text{dB}}$, which represents a usable frequency range, with the frequency response above -3 dB. $f_{3\text{dB}}$ is depicted by horizontal dashed lines in Fig. 2. Therefore, we calculate the dependence of bandwidth on τ_s , normalized by recombi-

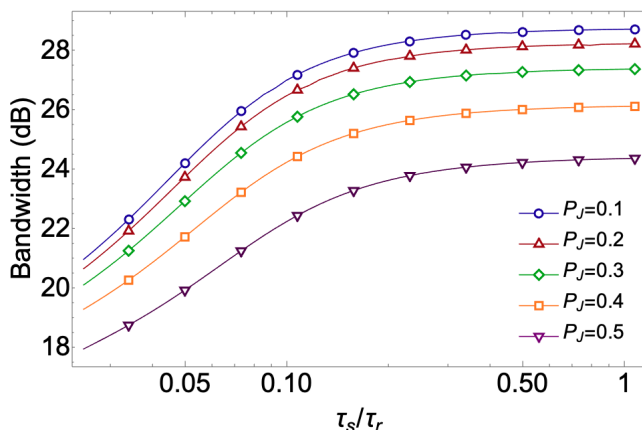


FIG. 3. The bandwidth dependence of the polarization response under AM with the normalized spin-relaxation time, τ_s/τ_r , for the polarization of injection, $P_J = 0.1$ to 0.5.

nation time τ_r . Even for the same gain material, τ_s/τ_r can strongly change with the growth direction [13, 49, 50], an applied gate voltage or magnetic field [20]. From the steady-state regime and at a fixed P_J [43], we can see several factors to generalize our AM description, focused on the analysis of the gain region, which is more accurate for the optical spin injection [6, 12–14, 16, 18], as electrical spin injection also involves spin-dependent transport from the injector. Both the lasing threshold reduction, as compared to the $P_J = 0$ limit, and the spin amplification, in which modest polarization of the carriers in the gain region yields a much larger P_S [13], depend on the τ_s/τ_r ratio [43]. This implies several additional AM mechanisms for δP_S . With strong transport nonlinearities in semiconductors there is a bias-dependent carrier polarization and P_S [20, 51–53]. An electrical spin injection in semiconductors and their light-emitting diodes can lead to both bias-dependent spin-relaxation time and the spin-dependent transport, for example, due to the barrier properties [20, 54–56]. A change in the applied bias could produce additional contributions to δP_S , to be included in Eqs. (6) and (7) and used in Eq. (9), or similar generalization beyond the simplified gain model.

We clearly see two trends in Fig. 3: the bandwidth increases with τ_s and decreases with P_J . The second trend appears counterintuitive since: (i) in conventional lasers an increase in $f_R = \omega_R/(2\pi)$ is related to the increase in the bandwidth, as expressed by $f_{3\text{dB}} \approx \sqrt{1 + \sqrt{2}}f_R$ [3] and (ii) from Eq. (4), as shown in the early of the AM in spin-lasers [30], that $f_R^- \propto \sqrt{(1 + |P_J|/2)(J_0/J_T - 1)}$. While (i) and (ii) would suggest that from an increase in f_R^- with P_J we should expect an *increase* in $f_{3\text{dB}}$ with P_J , both Figs. 2(b) and 3 reveal an opposite trend. Since ω_R^- , corresponding to the helicity light from the majority spin, becomes larger with P_J , while the ω_R^+ becomes smaller, there is a larger frequency separation between ω_R^{\pm} and lower response values. Consequently, at a smaller f , the response drops below -3 dB and $f_{3\text{dB}}$ is reduced. However, it does not mean that the smallest P_J would be ideal for a larger $f_{3\text{dB}}$. This is because the evaluation of $f_{3\text{dB}}$ includes a normalization. The actual value of δP_S decreases with P_J . For applications, δP_S should be large enough to be measurable and have a sufficient signal-to-noise ratio [30, 59, 60]. Therefore, an optimization between the magnitudes of P_J and $f_{3\text{dB}}$ is needed.

In addition to previously discussed analog operation, we can also examine the digital operation of spin-lasers, important for digital data transfer [3, 5]. Similar to conventional lasers, the corresponding AM is expressed as

$$J(t) = J_0 + \delta J(t) = J_0 + \delta J f(t), \quad (11)$$

where δJ is the modulation amplitude and, unlike our previously considered harmonic dependence, $f(t)$ is the binary function of the coded input signal. A binary “0” (“1”) is set to J_0 ($J_0 + \delta J$). In the previous AM studies

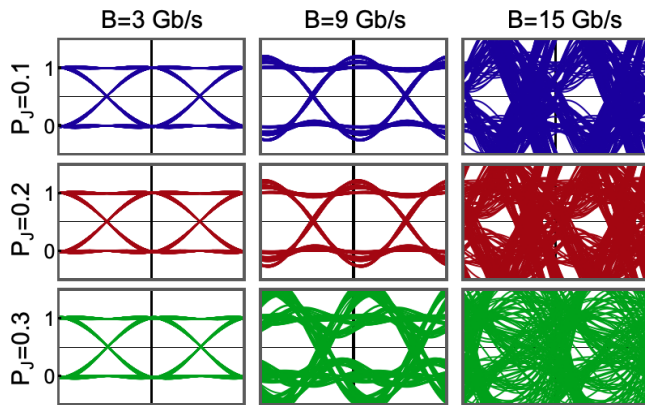


FIG. 4. Eye diagrams of a normalized polarization of the emitted light under AM for injection with $P_J = 0.1, 0.2,$ and $0.3,$ for a series of bit rates $B = 3, 9, 15$ Gb/s. Parameters: $J_0 = 3J_T,$ $\beta = 10^{-4},$ $\tau_s/\tau_r = 1.$

of conventional or spin-lasers, the emitted photon density would reflect the information encoded in the input $J(t)$ [3, 57]. Bit “0” (“1”) is then defined by being below (above) some specified threshold in S . However, here we focus on the polarization of the emitted light, such that “0” (“1”) is defined with respect to a threshold in P_S .

To analyze the quality of a digital signal, we use the eye diagrams. The size of the central “eye” opening indicates the distinguishability between digital “0” and “1” signals. We simulate a binary signal, by using 2^{10} pseudorandom bits with a common non-return-to-zero modulation, the pulse remains on throughout the bit slot, and its amplitude does not fall to zero between successive “1” bits. This stream of bits is first filtered by a generalized raised cosine filter [5] to reduce parasitic ringing effects which complicate distinguishing “0” and “1.”

The corresponding eye diagrams in Fig. 4 are generated by dividing the laser wave form into segments of an equal size of two bits and overlaying them. The bit slot time is an inverse of a bit rate, B . By separately changing these bit rates, $B = 3, 9, 15$ Gb/s, and the polarization injection, $P_J = 0.1, 0.2, 0.3,$ we can identify several trends for the digitally-encoded circular polarization under AM. We see that for a small polarization, $P_J = 0.1,$ the data transfer with a bit rate up to 15 Gb/s remain efficient. As P_J increases, the central eye in the diagrams starts to close, especially at large bit rates, indicating worse performance with $P_J.$

This trend in P_J is consistent with the behavior illustrated in Figs. 2(b) and 3, which both show a decreasing bandwidth with a larger $P_J.$ We note that the bit rate of open eye diagrams is smaller than the bandwidth. This can be understood because the time evolution of P_S depends not only on the separate amplitudes, S^+ and $S^-,$ but also on the phase differences between S^+ and $S^-,$ as shown by Eq. 10. From numerical calculations, we find that the phase difference depends on various factors

including $\omega,$ $B,$ and $P_J.$ In the eye diagrams, abrupt changes in the pseudorandom input with large bit rate leads to a transient effect [58], which influences the time-variation of the phase difference and the shape of $P_S.$ As a result, the maximum bit rate supporting open eye diagrams is suppressed, compared to the bandwidth in the response curves from Figs. 2(b) and 3.

With a simple amplitude modulation in spin-lasers, we have revealed overlooked nontrivial dynamics of their circularly polarized emitted light. Several identified trends have been corroborated by a combination of analytical and numerical methods, within the small signal analysis for both harmonic and digital modulation. Our findings, based on the rate-equation model in Eqs. (1) and (2), suggest several generalizations. One can combine this phenomenological approach with a microscopic gain calculation [34] and also include the hole spin-relaxation time, which could be important for GaN-based lasers [61], but was not considered in their experimental analysis [62]. Furthermore, it would be important to extend our findings to other types of rate-equation models which describe the effects of optical anisotropies [12, 63–69], or the presence of external cavities [14, 70].

Currently, dynamical room-temperature operation of VCSELs is limited to the optical injection of spin-polarized carriers [18]. Using the amplitude modulation is promising for the push towards their room-temperature operation with electrical spin injection. This effort could incorporate advances in ferromagnetic contacts with a perpendicular magnetization to remove the need for an applied magnetic field [22, 71, 72, 74–77]. Beyond the usual III-V gain regions, with a growing family of van der Waals materials, it could also be possible to combine a proposal for spin-lasers with an atomically-thin gain region [45], where the spin-polarized carriers would be provided by electrically-tunable magnetic proximity effects [28, 79].

For a full signal transduction between the carrier spin and the helicity of light, to enable versatile applications of spin-lasers for optical communication, high-performance interconnects, holographic information [80], or three-dimensional displays [24], another focus should be on the development of helicity detectors. Even for simple ferromagnetic contacts with GaAs, the optimization of such detectors requires a careful understanding of their dynamical properties [81].

We thank N. C. Gerhardt for valuable discussions. This work has been supported by the National Natural Science Foundation of China (Grant No. 12104118), the NSF ECCS-2130845, and AFOSR FA9550-22-1-0349.

AUTHOR DECLARATIONS

Conflict of interest

The authors have no conflicts to disclose.

DATA AVAILABILITY

The data that supports the findings of this study are available within the article.

* xug@hdu.edu.cn

† zigor@buffalo.edu

- [1] S. L. Chuang, *Physics of Optoelectronic Devices*, 2nd ed. (Wiley, New York, 2009).
- [2] L. A. Coldren, S. W. Corzine, and M. L. Mašović, *Diode Lasers and Photonic Integrated Circuits*, 2nd Edition (Wiley, Hoboken, 2012).
- [3] *VCSELs Fundamentals, Technology and Applications of Vertical-Cavity Surface-Emitting Lasers*, edited by R. Michalzik (Springer, Berlin, 2013).
- [4] R.-M. Ma and R. F. Oulton, Applications of nanolasers, *Nat. Nanotechnol.* **14**, 12 (2019).
- [5] G. P. Agrawal, *Fiber-Optic Communication Systems* (Wiley, New York, 2002).
- [6] J. Rudolph, D. Hägele, H. M. Gibbs, G. Khitrova, and M. Oestreich, Laser threshold reduction in a spintronic device, *Appl. Phys. Lett.* **82**, 4516 (2003).
- [7] J. Rudolph, S. Döhrmann, D. Hägele, M. Oestreich, and W. Stolz, Room-temperature threshold reduction in vertical-cavity surface-emitting lasers by injection of spin-polarized carriers, *Appl. Phys. Lett.* **87**, 241117 (2005).
- [8] M. Holub, J. Shin, and P. Bhattacharya, Electrical spin injection and threshold reduction in a semiconductor laser, *Phys. Rev. Lett.* **98**, 146603 (2007).
- [9] N. C. Gerhardt, S. Hövel, M. R. Hofmann, J. Yang, D. Reuter, A. Wieck, Enhancement of spin information with vertical cavity surface emitting lasers, *Electron. Lett.* **42**, 88 (2006).
- [10] S. Hövel, A. Bischoff, N. C. Gerhardt, M. R. Hofmann, T. Ackemann, A. Kroner, and R. Michalzik, Optical spin manipulation of electrically pumped vertical-cavity surface-emitting lasers, *Appl. Phys. Lett.* **92**, 041118 (2008).
- [11] D. Saha, D. Basu, and P. Bhattacharya, High-frequency dynamics of spin-polarized carriers and photons in a laser, *Phys. Rev. B* **82**, 205309 (2010).
- [12] N. C. Gerhardt, M. Y. Li, H. Jähme, H. Höpfner, T. Ackemann, and M. R. Hofmann, Ultrafast spin-induced polarization oscillations with tunable lifetime in vertical-cavity surface-emitting lasers, *Appl. Phys. Lett.* **99**, 151107 (2011).
- [13] S. Iba, S. Koh, K. Ikeda, and H. Kawaguchi, Room temperature circularly polarized lasing in an optically spin injected vertical-cavity surface-emitting laser with (110) GaAs quantum wells, *Appl. Phys. Lett.* **98**, 081113 (2011).
- [14] J. Frougier, G. Baili, M. Alouini, I. Sagnes, H. Y. Jaffrès, A. Garnache, C. Deranlot, D. Dolfi, and J.-M. George, Control of light polarization using optically spin-injected vertical external cavity surface emitting lasers, *Appl. Phys. Lett.* **103**, 252402 (2013).
- [15] J.-Y. Cheng, T.-M. Wond, C.-W. Chang, C.-Y. Dong, and Y.-F. Chen, Self-polarized spin-nanolasers, *Nat. Nanotechnol.* **9**, 845 (2014).
- [16] S. S. Alharthi, A. Hurtado, R. K. Al Seyab, V.-M. Korpjarvi, M. Guina, I. D. Henning, and M. J. Adams, Control of emitted light polarization in a 1310 nm dilute nitride spin-vertical cavity surface emitting laser subject to circularly polarized optical injection, *Appl. Phys. Lett.* **105**, 181106 (2014).
- [17] S. S. Alharthi, A. Hurtado, V.-M. Korpjarvi, M. Guina, I. D. Henning, and M. J. Adams, Circular polarization switching and bistability in an optically injected 1300 nm spin-vertical cavity surface emitting laser, *Appl. Phys. Lett.* **106**, 021117 (2015).
- [18] M. Lindemann, G. Xu, T. Pusch, R. Michalzik, M. R. Hofmann, I. Žutić, and N. C. Gerhardt, Ultrafast spin-lasers, *Nature* **568**, 212 (2019).
- [19] A. A. Maksimov, E. V. Filatov and I. I. Tartakovskii Temperature dependence of circularly polarized radiation of an injection semiconductor laser, *JETP Lett.* **116**, 500 (2022).
- [20] I. Žutić, J. Fabian, and S. Das Sarma, Spintronics: Fundamentals and applications, *Rev. Mod. Phys.* **76**, 323 (2004).
- [21] N. Nishizawa, K. Nishibayashi, and H. Munekata, Pure circular polarization electroluminescence at room temperature with spin-polarized light-emitting diodes, *Proc. Nat. Acad. Sci.* **114**, 1783 (2017).
- [22] I. Žutić, G. Xu, M. Lindemann, P. E. Faria Junior, J. Lee, V. Labinac, K. Stojšić, G. M. Sipahi, M. R. Hofmann, and N. C. Gerhardt, Spin-lasers: spintronics beyond magnetoresistance, *Solid State Commun.* **316-317**, 113949 (2020).
- [23] I. V. Rozhansky, V. N. Mantsevich, N. S. Maslova, P. I. Arseyev, N. S. Averkiev, and E. Lähderanta, Ultrafast electrical control of optical polarization in hybrid semiconductor structure, *Physica E* **132**, 114755 (2021).
- [24] N. Nishizawa and H. Munekata, Lateral-type spin-photonics devices: Development and applications, *Micromachines* **12**, 644 (2021).
- [25] E. Y. Tsybmal and I. Žutić (eds.), *Spintronics Handbook: Spin Transport and Magnetism*, 2nd ed. (CRC Press, Boca Raton, FL 2019).
- [26] H. Dery, Y. Song, P. Li, and I. Žutić, Silicon spin communication, *Appl. Phys. Lett.* **99**, 082502 (2011).
- [27] A. Khaetskii, V. N. Golovach, X. Hu, and I. Žutić, Proposal for a phonon laser utilizing quantum-dot spin states, *Phys. Rev. Lett.* **111**, 186601 (2013).
- [28] I. Žutić, A. Matos-Abiague, B. Scharf, H. Dery, and K. Belashchenko, Proximitized materials, *Mater. Today* **22**, 85 (2019).
- [29] N. Yokota, and K. Nisaka, H. Yasaka, and K. Ikeda, Spin polarization modulation for high-speed vertical-cavity surface-emitting lasers, *Appl. Phys. Lett.* **113**, 171102 (2018).
- [30] J. Lee, W. Falls, R. Oszwaldowski, and I. Žutić, Spin modulation in lasers, *Appl. Phys. Lett.* **97**, 041116 (2010).
- [31] M. Drong, T. Fördös, H. Y. Jaffrès, J. Peřina Jr., K. Postava, P. Ciompa, J. Piřtora, and H.-J. Drouhin, Spin-

- VCSELs with local optical anisotropies: Toward terahertz polarization modulation, *Phys. Rev. Applied* **15**, 014041 (2021).
- [32] Y. Huang, P. Zhou, M. S. Torre, N. Li, I. D. Henning, and M. J. Adams, Optically pumped spin-VCSELs: Toward high-frequency polarization oscillations and modulation, *IEEE J. Quant. Electron.* **57**, 2400212 (2021).
- [33] N. Heermeier, T. Heuser, J. Große, N. Jung, A. Kagan-skiy, M. Lindemann, N. C. Gerhardt, M. R. Hofmann, and S. Reitzenstein, Spin-lasing in bimodal quantum dot micropillar cavities, *Laser Photonics Rev.* **16**, 2100585 (2022).
- [34] P. E. Faria Junior, G. Xu, J. Lee, N. C. Gerhardt, G. M. Sipahi, and I. Žutić, Towards high-frequency operation of spin-lasers, *Phys. Rev. B* **92**, 075311 (2015).
- [35] M. Lindemann, T. Pusch, R. Michalzik, N. C. Gerhardt, and M. R. Hofmann, Frequency tuning of polarization oscillations: Toward high-speed spin-lasers, *Appl. Phys. Lett.* **108**, 042404 (2016).
- [36] T. Pusch, M. Lindemann, N. C. Gerhardt, M. R. Hofmann, and R. Michalzik, Vertical-cavity surface-emitting lasers with birefringence above 250 GHz, *Electron. Lett.* **51**, 1600 (2015).
- [37] T. Pusch, E. La Tona, M. Lindemann, N. C. Gerhardt, M. R. Hofmann, and R. Michalzik, Monolithic vertical-cavity surface-emitting laser with thermally tunable birefringence, *Appl. Phys. Lett.* **110**, 151106 (2017).
- [38] T. Pusch, P. Debernardi, M. Lindemann, F. Erb, N. C. Gerhardt, M. R. Hofmann and R. Michalzik, Vertical-cavity surface-emitting laser with integrated surface grating for high birefringence splitting *Electron. Lett.* **55**, 1055 (2019).
- [39] T. Fördös, H. Y. Jaffrès, K. Postava, M. S. Seghilani, A. Garnache, J. Pistora, and H. J. Drouhin, Eigenmodes of spin vertical-cavity surface-emitting lasers with local linear birefringence and gain dichroism, *Phys. Rev. A* **96**, 043828 (2017).
- [40] N. Yokota and H. Yasaka, Spin laser local oscillators for homodyne detection in coherent optical communications, *Micromachines* **12**, 573 (2021).
- [41] C. Tselios, P. Georgiou, C. Politi, and D. Alexandropoulos Polarization control of quantum-dot spin-VCSELs, *Phys. Stat. Solidi B* **259**, 2100532 (2022)
- [42] D. Basu, D. Saha and P. Bhattacharya, Optical polarization modulation and gain anisotropy in an electrically injected spin laser, *Phys. Rev. Lett.* **102**, 093904 (2009).
- [43] C. Gøthgen, R. Oszwałdowski, A. Petrou, and I. Žutić, Analytical model of spin-polarized semiconductor lasers, *Appl. Phys. Lett.* **93**, 042513 (2008).
- [44] J. Lee, R. Oszwałdowski, C. Gøthgen, and I. Žutić, Mapping between quantum dot and quantum well lasers: From conventional to spin lasers, *Phys. Rev. B* **85**, 045314 (2012).
- [45] J. Lee, S. Bearden, E. Wasner, and I. Žutić, Spin-lasers: From threshold reduction to large-signal analysis, *Appl. Phys. Lett.* **105**, 042411 (2014).
- [46] G. Bourdon, I. Robert, I. Sagnes, and I. Abram, Spontaneous emission in highly excited semiconductors: Saturation of the radiative recombination rate, *J. Appl. Phys.* **92**, 6595 (2002). The linear form is obvious for $T = 0$ K and $n = p$, where the density of electron-hole pairs that can recombine is n .
- [47] J. Hader, J. V. Moloney, and S. W. Koch, Beyond the ABC: carrier recombination in semiconductor lasers, *Proc. SPIE* **6115**, 61151T (2006). The precise functional form of the carrier recombination changes with density. At higher densities, commonly considered quadratic recombination, Bn^2 , attains a linear form, Bn .
- [48] G. Xu, K. Patel, and I. Žutić, Threshold behavior in spin lasers: Spontaneous emission and nonlinear gain, *Appl. Phys. Lett.* **119**, 171104 (2021).
- [49] S. Iba, Y. Ohno, and H. Saito, Recent progress on crystal growth of high-quality (110)GaAs-based quantum wells for spin laser, *Proc. SPIE* **11470**, 114702P (2020).
- [50] Y. Ohno, S. Iba, R. Okamoto, Y. Obata, K. Obu, J. J. Pascual Domingez, and H. Saito, Room-temperature spin relaxation in a (110)-oriented GaAs/AlGaAs superlattice with tunnel-coupled quantum wells, *Appl. Phys. Express* **13**, 123003 (2022).
- [51] I. Žutić, J. Fabian, and S. Das Sarma, Spin injection through the depletion layer: A theory of spin-polarized p - n junctions and solar cells, *Phys. Rev. B* **64**, 121201(R) (2001).
- [52] I. Žutić, J. Fabian, and S. Das Sarma, Spin-polarized transport in inhomogeneous magnetic semiconductors: Theory of magnetic/nonmagnetic p - n junctions, *Phys. Rev. Lett.* **88**, 066603 (2002).
- [53] I. Žutić, J. Fabian, and S. C. Erwin, Bipolar spintronics: From spin injection to spin-controlled logic, *J. Phys.: Condens. Matter* **19**, 165219 (2007).
- [54] A. E. Giba, X. Gao, M. Stoffel, X. Devaux, B. Xu, X. Marie, P. Renucci, H. Jaffrès, J.-M. George, G. Cong, Z. Wang, H. Rinnert, and Y. Lu, Spin injection and relaxation in p-doped (In,Ga)As/GaAs quantum-dot spin light-emitting diodes at zero magnetic field, *Phys. Rev. Applied* **14**, 034017 (2020).
- [55] P. Barate, S. H. Liang, T. T. Zhang, J. Frougier, B. Xu, P. Schieffer, M. Vidal, H. Jaffrès, B. Lépine, S. Tricot, F. Cadiz, T. Garandel, J. M. George, T. Amand, X. Devaux, M. Hehn, S. Mangin, B. Tao, X. F. Han, Z. G. Wang, X. Marie, Y. Lu, and P. Renucci, Bias dependence of the electrical spin injection into GaAs from Co-Fe-B/MgO injectors with different MgO growth processes, *Phys. Rev. Applied* **8**, 054027 (2017).
- [56] S. A. Crooker, E. S. Garlid, A. N. Chantis, D. L. Smith, K. S. M. Reddy, Q. O. Hu, T. Kondo, C. J. Palmström, and P. A. Crowell, Bias-controlled sensitivity of ferromagnet/semiconductor electrical spin detectors, *Phys. Rev. B* **80**, 041305(R) (2009).
- [57] E. Wasner, S. Bearden, J. Lee, and I. Žutić, Digital operation and eye diagrams in spin-lasers, *Appl. Phys. Lett.* **107**, 082406 (2015).
- [58] G. Boéris, J. Lee, K. Výborný, and I. Žutić, Tailoring chirp in spin-lasers, *Appl. Phys. Lett.* **100**, 121111 (2012).
- [59] T. Wang, J. Zou, G. P. Puccioni, W. Zhao, X. Lin, H. Chen, G. Wang, and G. L. Lippi, Methodological investigation into the noise influence on nanolasers' large signal modulation, *Opt. Express* **29**, 5081 (2021).
- [60] X. Li, H. Wang, Z. Qiao, J. X. B. Sia, W. Wang, X. Guo, Y. Zhang, Z. Niu, C. Tong, and C. Liu, Temperature-dependent phase noise properties of a two-section GaSb-based mode-locked laser emitting at 2 μ m, *Appl. Phys. Lett.* **117**, 141103 (2020).
- [61] P. E. Faria Junior, G. Xu, Y.-F. Chen, G. M. Sipahi, and I. Žutić, Wurtzite spin lasers, *Phys. Rev. B* **95**, 115301 (2017).

- [62] A. Bhattacharya, M. Zunaid Baten, I. Iorsh, T. Frost, A. Kavokin, and P. Bhattacharya, Room-temperature spin polariton diode laser, *Phys. Rev. Lett.* **119**, 067701 (2017).
- [63] M. San Miguel, Q. Feng, and J. V. Moloney, Light-polarization dynamics in surface-emitting semiconductor lasers, *Phys. Rev. A* **52**, 1728 (1995).
- [64] A. Dyson and M. J. Adams, Spin-polarized properties of optically pumped vertical cavity surface emitting lasers, *J. Opt. B, Quantum Semiclass. Opt.* **5**, 222 (2003).
- [65] M. Adams, N. Li, B. Cemlyn, H. Susanto, and I. Henning, Algebraic expressions for the polarisation response of spin-VCSELs, *Semicond. Sci. Technol.* **33**, 064002 (2018).
- [66] G. Xu, J. D. Cao, V. Labinac, and I. Žutić, Intensity equations for birefringent spin lasers, *Phys. Rev. B* **103**, 045306 (2021).
- [67] M. Adams, N. Li, Yu Huang, P. Zhou, and I. Henning, Three-variable reduction of the spin-flip model for spin-VCSELs, *IEEE J. Quant. Electron.* **58**, 2400308 (2022).
- [68] N. Yokota, K. Ikeda, and H. Yasaka, Observation of spin polarization modulation responses of injection-locked vertical-cavity surface-emitting lasers, *IEICE Electron. Express* **20**, 20230057 (2023).
- [69] K. Panajotov, M. Petrov, and Y. Marinov, Liquid-crystal spin-VCSEL with electro-optically controllable birefringence *Photonics* **10**, 179 (2023).
- [70] M. Alouini, J. Frougier, A. Joly, G. Baïli, D. Dolfi, and J.-M. Georges, VSPIN: A new model relying on the vectorial description of the laser field for predicting the polarization dynamics of spin-injected V(e)CSELs, *Opt. Express* **26**, 6739 (2018).
- [71] A. Sinsarp, T. Manago, F. Takano, and H. Akinaga, Electrical spin injection from out-of-plane magnetized FePt/MgO tunneling junction into GaAs at room temperature, *Jpn. J. Appl. Phys.* **46**, L4 (2007).
- [72] S. Hövel, N.C. Gerhardt, M.R. Hofmann, F.-Y. Lo, A. Ludwig, D. Reuter, A.D. Wieck, E. Schuster, H. Wende, W. Keune, O. Petracic, and K. Westerholt, Room temperature electrical spin injection in remanence, *Appl. Phys. Lett.* **93**, 021117 (2008).
- [73] J. Zarpellon, H. Jaffres, J. Frougier, C. Deranlot, J. M. George, D. H. Mosca, A. Lemaitre, F. Freimuth, Q. H. Duong, P. Renucci, and X. Marie, Spin injection at remanence into III-V spin light-emitting diodes using (Co/Pt) ferromagnetic injectors, *Phys. Rev. B* **86**, 205314 (2012).
- [74] S. H. Liang, T. T. Zhang, P. Barate, J. Frougier, M. Vidal, P. Renucci, B. Xu, H. Jaffrés, J.-M. George, X. Devaux, M. Hehn, X. Marie, S. Mangin, H. X. Yang, A. Hallal, M. Chshiev, T. Amand, H. F. Liu, D. P. Liu, X. F. Han, Z. G. Wang, and Y. Lu, Large and robust electrical spin injection into GaAs at zero magnetic field using an ultrathin CoFeB/MgO injector, *Phys. Rev. B* **90**, 085310 (2014).
- [75] A. E. Giba, X. Gao, M. Stoffel, X. Devaux, B. Xu, X. Marie, P. Renucci, H. Jaffrés, J.-M. George, G. Cong, Z. Wang, H. Rinnert, and Y. Lu, Spin injection and relaxation in p-doped (In,Ga)As/GaAs quantum-dot spin light-emitting diode at zero magnetic field, *Phys. Rev. Appl.* **14**, 034017 (2020).
- [76] B. Tao, P. Barate, X. Devaux, P. Renucci, J. Frougier, A. Djéffal, S. Liang, Bo Xu, M. Hehn, H. Jaffrés, J.-M. George, X. Marie, S. Mangin, X. Han, Z. Wang, and Y. Lu, Atomic-scale understanding of high thermal stability of Mo/CoFeB/MgO spin injector for spin-injection in remanence, *Nanoscale* **10**, 10213 (2018).
- [77] F. Cadiz, A. Djéffal, D. Lagarde, A. Balocchi, B. S. Tao, B. Xu, S.H. Liang, M. Stoffel, X. Devaux, H. Jaffrés, J.-M. George, M. Hehn, S. Mangin, H. Carrere, X. Marie, T. Amand, X. F. Han, Z. G. Wang, B. Urbaszek, Y. Lu, and P. Renucci, Electrical initialization of electron and nuclear spins in a single quantum dot at zero magnetic field, *Nano Lett.* **18**, 2381 (2018).
- [78] I. Žutić, A. Matos-Abiague, B. Scharf, H. Dery, and K. Belashchenko, Proximitized materials, *Mater. Today* **22**, 85 (2019).
- [79] S. Liang, T. Xie, N. A. Blumenschein, T. Zhou, T. Ersevrim, Z. Song, J. Liang, M. A. Susner, B. S. Conner, S.-J. Gong, J.-P. Wang, M. Ouyang, I. Žutić, A. L. Friedman, X. Zhang, and C. Gong, Small-voltage multiferroic control of two-dimensional magnetic insulators, *Nat. Electron.* **6**, 199 (2023).
- [80] P.-N. Ni, P. Fu, P.-P. Chen, C. Xu, Y.-Y. Xie, and P. Geneve, Spin-decoupling of vertical cavity surface-emitting lasers with complete phase modulation using on-chip integrated Jones matrix metasurfaces, *Nat. Commun.* **13**, 7795 (2022).
- [81] V. I. Safarov, I. V. Rozhansky, Z. Zhou, B. Xu, Z.-M. Wei, Z.-G. Wang, Y. Lu, H. Jaffrés, and H.-J. Drouhin, Recombination times mismatch and spin dependent photocurrent at a ferromagnetic-metal/semiconductor tunnel junction, *Phys. Rev. Lett.* **128**, 057701 (2022).